Arts, Karsten; Thepass, Harvey; Verheijen, Marcel A.; Puurunen, Riikka L.; Kessels, Wilhelmus M.M.; Knoops, Harm C.M.

Impact of Ions on Film Conformality and Crystallinity during Plasma-Assisted Atomic Layer Deposition of TiO_2

Published in:
Chemistry of Materials

DOI:
10.1021/acs.chemmater.1c00781

Published: 13/07/2021

Document Version
Publisher's PDF, also known as Version of record

Please cite the original version:
Arts, K., Thepass, H., Verheijen, M. A., Puurunen, R. L., Kessels, W. M. M., & Knoops, H. C. M. (2021). Impact of Ions on Film Conformality and Crystallinity during Plasma-Assisted Atomic Layer Deposition of TiO_2. *Chemistry of Materials*, *33*(13), 5002–5009. https://doi.org/10.1021/acs.chemmater.1c00781

CHEMISTRY OF MATERIALS

pubs.acs.org/cm

Article

Impact of Ions on Film Conformality and Crystallinity during Plasma-Assisted Atomic Layer Deposition of TiO_2

Karsten Arts, Harvey Thepass, Marcel A. Verheijen, Riikka L. Puurunen, Wilhelmus M. M. Kessels,* and Harm C. M. Knoops*

Cite This: *Chem. Mater.* 2021, 33, 5002−5009

Read Online

ACCESS | Metrics & More | Article Recommendations | Supporting Information

ABSTRACT: This work demonstrates that ions have a strong impact on the growth per cycle (GPC) and material properties during plasma-assisted atomic layer deposition (ALD) of TiO_2 (titanium dioxide), even under mild plasma conditions with low-energy (<20 eV) ions. Using vertical trench nanostructures and microscopic cavity structures that locally block the flux of ions, it is observed that the impact of (low-energy) ions is an important factor for the TiO_2 film conformality. Specifically, it is demonstrated that the GPC in terms of film thickness can increase by 20 to >200% under the influence of ions, which is correlated with an increase in film crystallinity and an associated strong reduction in the wet etch rate (in 30:1 buffered HF). The magnitude of the influence of ions is observed to depend on multiple parameters such as the deposition temperature, plasma exposure time, and ion energy, which may all be used to minimize or exploit this effect. For example, a relatively moderate influence of ions is observed at 200 °C when using short plasma steps and a grounded substrate, providing a low ion-energy dose of ~1 eV nm^{-2} $cycle^{-1}$, while a high effect is obtained when using extended plasma exposures or substrate biasing (~100 eV nm^{-2} $cycle^{-1}$). This work on TiO_2 shows that detailed insight into the role of ions during plasma ALD is essential for precisely controlling the film conformality, material properties, and process reproducibility.

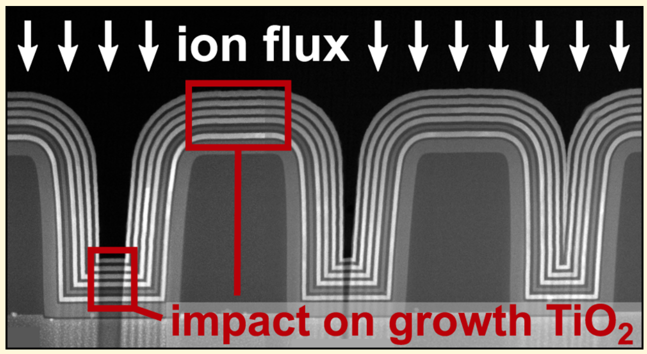

■ INTRODUCTION

Titanium oxide is a widely studied material and as a thin film has many applications,[1] such as in photocatalysis,[2] photonics,[3−5] photovoltaics,[6] and nanoelectronics,[7] where in the latter, TiO_2 primarily functions as high-k dielectric. Especially in the field of nanoelectronics, the miniaturization of device structures has strongly increased the demand for atomic-scale processing techniques such as (plasma-assisted) atomic layer deposition (ALD), which can typically provide atomic-level thickness control.[8−10] In the case of TiO_2, ALD is used, for instance, in self-aligned multiple patterning for the preparation of nanometer-thin TiO_2 sidewall spacers.[11,12] Furthermore, plasma ALD of TiO_2 has been reported for gap-filling and encapsulation applications in the fabrication of memory devices such as dynamic random-access memory (DRAM), where a high level of TiO_2 film conformality is required to isolate adjacent memory cells.[13]

In previous work, we demonstrated that plasma ALD of TiO_2 can fully penetrate into horizontally oriented trench structures with extremely high aspect ratio (AR) values of ~800.[14,15] This indicates that excellent TiO_2 film conformality can be achieved, which is enabled by a low loss of reactive radicals on the TiO_2 surface.[14,15] However, it is possible that the film conformality is still reduced by any influence of ions, which were not taken into account in our previous study employing the horizontal trench structures.[16] Even though ions often have a beneficial effect,[17−20] the flux of ions on surfaces is inherently anisotropic and can therefore induce nonuniform growth behavior on a three-dimensional (3D) surface topography.[19]

The influence of ions on plasma ALD of TiO_2 has been explored, for instance, by Profijt et al.[17] and Faraz et al.,[19] by greatly increasing the energy of the ions (e.g., to 100−200 eV) through external substrate biasing. For example, it has been shown that high-energy ions can be used to tune the properties of the deposited TiO_2 such as the crystalline phase, film density, residual stress, and refractive index.[17,19] These are all important for controlling application-relevant parameters, such as the optical properties,[3−5] etch resistance,[11,12] and catalytic activity.[2] Here, using $Ti(NMe_2)_4$ as a precursor, we demonstrate that also ions with low energies of <20 eV, as

Received: March 3, 2021
Revised: April 15, 2021
Published: April 29, 2021

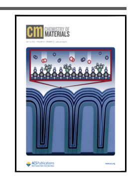

typical during plasma ALD processes,[9,20] have a crucial impact on plasma ALD of TiO_2.

By investigating film growth with exposure to ions and without any contribution of ions, we reveal that the influence of ions is significant even under mild plasma conditions and when using a grounded substrate. This influence is verified to significantly affect the film conformality obtained on 3D nanostructures. Moreover, the growth per cycle (GPC) is observed to be highly susceptible to the influence of (low-energy) ions. This can be an important factor behind the large spread in GPC values reported in the literature[19,21−29] for this process (see the Supporting Information). Therefore, detailed information on the influence of ions may be essential for improving the limited reproducibility of plasma ALD of TiO_2 in between labs and ALD tools, which appears to be a long-standing issue. In addition to the GPC, the influence of ions on the crystallinity of the TiO_2 is investigated since the crystallinity can have a strong effect on the ALD growth behavior[30,31] and on material properties such as the wet etch rate and the refractive index. Finally, the impact of ions is studied at various deposition temperatures and plasma exposure times to explore under what conditions this impact can either be minimized or exploited.

EXPERIMENTAL METHOD

The impact of ion exposure during plasma ALD of TiO_2 has been investigated using microscopic lateral-high-aspect-ratio (LHAR) trench structures (PillarHall generation 4),[32−34] where only part of the growth area is exposed to ions.[16] A top-view microscope image and schematic cross-sectional side-view images of the LHAR structures are provided in Figure 1. In these all-silicon structures, a

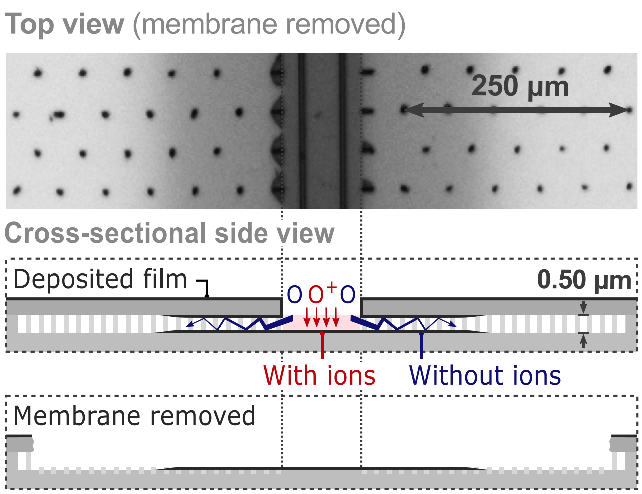

Figure 1. Top-view microscope image and schematic cross-sectional side-view images of PillarHall LHAR cavity structures[32−34] used in this work to study plasma ALD of TiO_2 with exposure to ions (opening) and without any contribution of ions (cavity).

horizontally oriented cavity with an extremely high AR is formed by a surface over which a membrane is suspended that is supported by a network of pillars with a nominal gap height of 500 nm. During deposition, the anisotropic ions only impinge on the surface in the plasma-exposed region that is not covered by the membrane. In contrast, the plasma radicals are supplied to the exposed and shielded regions, as they can diffuse deep into the cavity.[14]

In our experiments, the ion-shielding membrane of each LHAR structure was removed after deposition using adhesive tape. Subsequently, the thickness of the film grown with and without exposure to ions, as plotted in Figure 3C in terms of the local GPC, was measured using optical reflectometry (Filmetrics F40-UV with a StageBase-XY10-Auto-100mm mapping stage). The film thickness was fitted assuming a refractive index of 2.49 at 633 nm for TiO_2, as confirmed by spectroscopic ellipsometry (SE). The assumption of a constant refractive index for all conditions is not perfect but has a relatively minor influence on the accuracy of the thickness measurement. In addition to the GPC, the local wet etch rate was determined by measuring the thickness profile before and after a 7 min etch in 30:1 buffered HF at room temperature, with NH_4F as the buffer agent. For all reflectometry measurements of the GPC and the wet etch rate, the thickness (and optical properties) of the TiO_2 grown with exposure to ions was verified using ex situ SE. These measurements were performed on Si reference samples that were processed alongside the corresponding LHAR structures (see the Supporting Information for the used SE model and hardware). Finally, the crystallinity of TiO_2 was investigated by Raman spectroscopy using an Invia confocal Raman microscope of Renishaw.

In addition to the studies using LHAR structures, the impact of ions on the TiO_2 film conformality has been evaluated using more traditional, vertically oriented trench nanostructures with different ARs in the range of approximately 1−10.[19,35] The coupon containing these trench nanostructures was prepared and provided by Lam Research. A cross-sectional analysis of the acquired film conformality was carried out using high-angle annular dark-field scanning transmission electron microscopy (HAADF-STEM) and energy-dispersive X-ray spectroscopy (EDS), both using a JEOL ARM 2010F. The TEM sample was prepared by a standard focused ion beam (FIB) lift-out scheme after coating the processed coupon with a protective spin-on epoxy layer.

All depositions were carried out using an Oxford Instruments FlexAL ALD reactor, equipped with a remote inductively coupled plasma (ICP) source operated at 13.56 MHz.[36] For the O_2/Ar plasma half-cycles, 100 sccm O_2 flow, 50 sccm Ar flow, 50 mTorr pressure, 600 W ICP power, and a grounded substrate were used. This provided a relatively low ion flux and energy of $\sim 10^{13}$ cm^{-2} s^{-1} and 9 ± 1 eV average (see Figure 2), as measured using a retarding field energy analyzer (RFEA) (Semion sensor of Impedans Ltd.). In addition, in one deposition run, 60 W substrate biasing was used, supplied by an RF power supply through an automatic matching unit. As measured using an RFEA, this gives a high mean ion energy of ∼120 eV during all plasma steps of this deposition run.

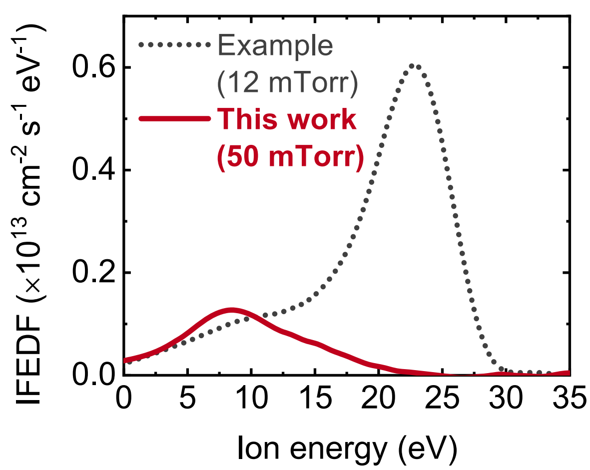

Figure 2. Ion flux-energy distribution function (IFEDF)[20] of the O_2/Ar plasma employed in this work (solid line). The plasma was generated at a pressure of 50 mTorr, using 600 W ICP power and a grounded substrate, providing a low mean ion energy of 9 ± 1 eV and an ion flux of $\sim 10^{13}$ cm^{-2} s^{-1} (peak area). As a comparison, the IFEDF of O_2/Ar plasma generated at a pressure of 12 mTorr is also shown (dotted line).

https://doi.org/10.1021/acs.chemmater.1c00781
Chem. Mater. 2021, 33, 5002−5009

The precursor $Ti(NMe_2)_4$ (tetrakis(dimethylamino)titanium, TDMAT) was used for the growth of TiO_2. In addition, $SiH_2(NEt_2)_2$ (bis(diethylamino)silane, BDEAS) and $AlMe_3$ (trimethylaluminum, TMA) were used for growing SiO_2 and Al_2O_3, respectively, which served as benchmark materials for comparing the influence of ions. In all recipes, high precursor doses were used such that the film penetration into the LHAR structures was typically limited by the plasma steps.[14] Unless stated otherwise, all depositions were carried out using 400 ALD cycles. To study the influence of ions at different conditions, the TiO_2 depositions were carried out at set table temperatures of 100, 200, and 300 °C, with a chamber wall temperature of 145 °C (or 100 °C for the table temperature setpoint of 100 °C). Due to limited thermal contact between the substrate and the table, these temperature setpoints corresponded to estimated substrate temperatures of 100, 180, and 240 °C. Finally, the influence of the ion dose was studied using different plasma exposure times of either 3.8, 12, 38, or 120 s per ALD cycle.

RESULTS AND DISCUSSION

Here, the results obtained using the aforementioned experimental approaches are presented. First, the impact of ions on film conformality during plasma ALD of TiO_2 is discussed. The results are benchmarked against the film conformality obtained during plasma ALD of SiO_2, where low-energy ions also have a significant influence.[16] Moreover, the results are compared to plasma ALD of Al_2O_3 to illustrate that, specifically for plasma ALD of TiO_2 and SiO_2, the influence of ions on film conformality is typically stronger than the influence of radical recombination (which is described in our earlier publications[14,15,37]). Second, the impact of ions on the TiO_2 material properties (i.e., crystallinity and wet etch rate) and GPC is investigated at different deposition temperatures and plasma exposure times.

Film Conformality: Benchmark against Plasma ALD of SiO_2. The impact of ions on plasma ALD of TiO_2 was first investigated using LHAR cavity structures, of which a schematic cross-sectional side view is given in panel A of Figure 3. Panel B shows top-view optical microscopy images of the LHAR structures after deposition and removal of the ion-shielding membrane. The TiO_2 and SiO_2 films (deposited using a table temperature of 200 °C, plasma steps of 12 s, and a grounded substrate) are visible in panel B due to optical thin-film interference. Finally, panel C shows the local GPC (the average over 400 cycles) in terms of film thickness as a function of distance into the LHAR structures.

Two key results are provided in Figure 3. First of all, deposition by reactive neutrals is achieved up to a distance of ~250 μm, corresponding to an extremely high AR value of ~500, with a relatively limited decrease in thickness with distance into the cavity. This confirms that excellent film conformality can be achieved for both materials, as reported in our earlier work.[14,15] Yet, Figure 3 also demonstrates that for both processes, the film growth is significantly influenced by ions. This is seen, for instance, in the top-view optical microscopy images (panel B), where the surface areas in the ion-exposed regions have a different darkness compared to the shielded cavity regions (i.e., darker for TiO_2 and lighter for SiO_2). Panel C shows that the difference in darkness corresponds to a significantly higher GPC for TiO_2, while the GPC for plasma ALD of SiO_2 is reduced upon exposure to ions.[16] The observed impact of (low-energy) ions suggests that ions can significantly influence film conformality during plasma ALD of TiO_2 and SiO_2, as the flux of ions is directional and can therefore cause nonuniform growth on a 3D structure. To assess to what extent the influence of ions is also observed on traditional, vertically oriented trench structures with relatively low ARs of <10, a case study was carried out, as shown in Figure 4.

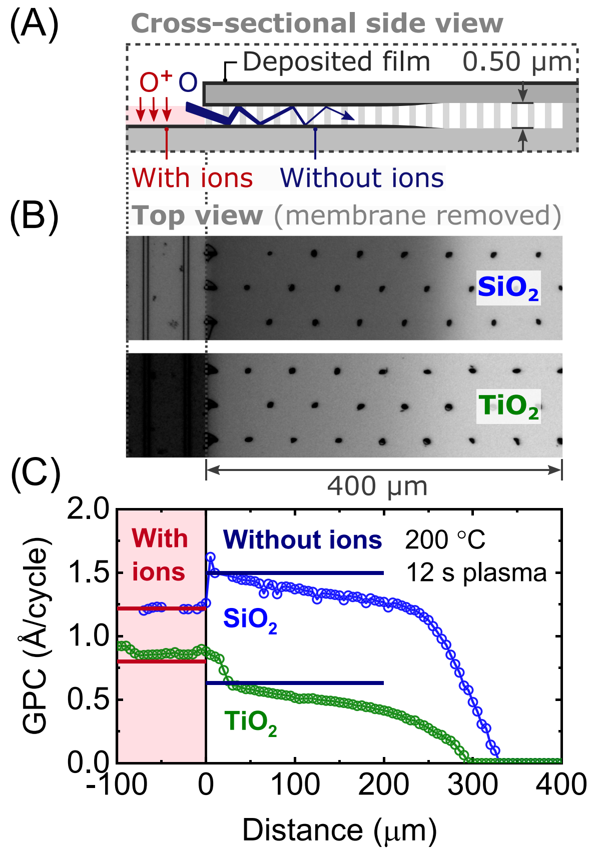

Figure 3. Schematic side view (A) of LHAR cavity structures used to study plasma ALD of SiO_2 and TiO_2 with (left) and without (right) exposure to (low-energy) ions. Examples of deposited films are visible in the top-view optical microscopy images (B), where the ion-shielding membrane is removed. The reflectometry data given in panel C indicate that the GPC obtained with exposure to ions (left) is significantly higher for TiO_2 and lower for SiO_2 compared to the GPC obtained without any contribution of ions (right). The values obtained with exposure to ions are confirmed by spectroscopic ellipsometry (red, horizontal bars).

Figure 4 shows cross-sectional TEM images (panels A and C) and an elemental map by EDS (panel B) of a stack of alternated layers of TiO_2 and SiO_2, deposited by plasma ALD on vertical trenches with different ARs. Each TiO_2 layer was grown using 140 cycles and each SiO_2 layer using 70 cycles. Additionally, a single layer of Al_2O_3 is included, also grown by plasma ALD using 70 cycles. Throughout the deposition of the stack, the same conditions were used as in Figure 3 (i.e., a table temperature of 200 °C, plasma steps of 12 s, and a grounded substrate). While panels A and B demonstrate conformal and seamless gap-filling by plasma ALD of TiO_2 and SiO_2, a closer inspection does reveal that the film conformality is indeed influenced by ions. This influence is quantified in panel D, where the average GPC is plotted for the TiO_2 and SiO_2 layers grown at the different locations indicated in panel C. For TiO_2, the GPC obtained on surfaces that are directly exposed to ions (i.e., the planar bottom and top surfaces) is again higher than the GPC on surfaces with limited exposure to ions (i.e., the

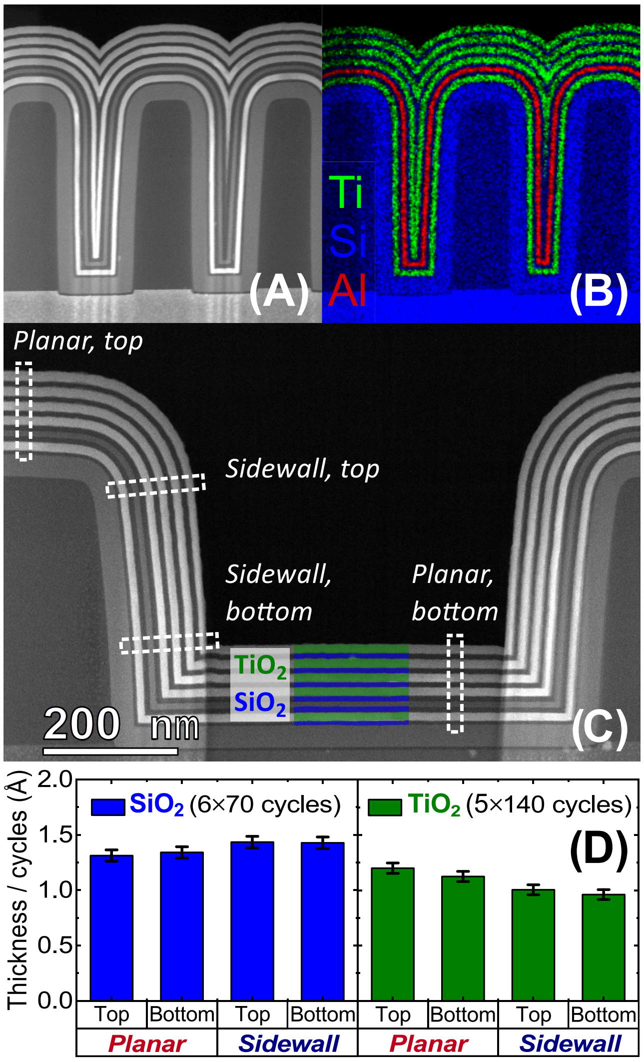

Figure 4. Cross-sectional HAADF-STEM images (A, C) and an EDS map (B) of a stack of alternated TiO_2 and SiO_2 layers and a single layer of Al_2O_3, deposited on vertical trenches with different initial aspect ratios of approximately 4.3 (A, left), 5.6 (A, right), and 0.6 (C). All layers are grown at 200 °C using plasma steps of 12 s. Panel D gives the GPC values corresponding to the TiO_2 and SiO_2 layers grown at the different locations indicated in panel C (excluding the first SiO_2 layer), demonstrating a similar influence of ions, as observed in Figure 3 using LHAR cavity structures.

sidewalls). For SiO_2, the opposite is observed, where the GPC is lower on the ion-exposed surfaces.

The results presented in Figure 4 illustrate that any influence of (low-energy) ions can to a certain extent compromise film conformality during plasma ALD in general. Another factor that often limits film conformality during plasma ALD is the loss of reactive radicals through recombination at surfaces.[14,15,37] This loss mechanism typically limits the AR up to which film growth by plasma ALD is feasible.[14,15,37] Compared to plasma ALD of TiO_2 and SiO_2, surface recombination of oxygen radicals is much more significant in the case of plasma ALD of Al_2O_3.[14] Nevertheless, for the fairly low ARs used, panels A and B reveal that also for plasma ALD of Al_2O_3, a highly conformal film is obtained even in the narrowest trench, indicating that the impact of radical recombination was negligible. Similarly, the results obtained in Figure 3 for TiO_2 and SiO_2 also indicate a negligible influence of radical recombination, as relatively conformal film growth by radicals was achieved up to extremely high AR values of ~500.[14] Specifically for plasma ALD of TiO_2 and SiO_2, film conformality is thus mostly influenced by the impact of ions (under the representative conditions used), rather than by surface recombination of reactive radicals.

Film Crystallinity and the Influence of Process Conditions. In addition to the film thickness, low-energy ions can also influence the properties of the deposited TiO_2. This has also been studied using the LHAR structures. For this purpose, TiO_2 depositions were carried out at table temperature setpoints of 100, 200, and 300 °C, using plasma steps of 38 s and the same plasma conditions as before (i.e., a grounded substrate and a mean ion energy of 9 ± 1 eV). Additionally, at a table temperature of 200 °C, a deposition run was carried out using plasma steps of 12 s and 60 W substrate biasing, giving a high mean ion energy of ~120 eV.

The crystallinity of the deposited TiO_2, which was investigated using Raman spectroscopy, can have a large impact on material properties such as the refractive index[19] as well as on the ALD growth behavior.[30,31] Examples of Raman spectra are presented in Figure 5, which are all measured in the

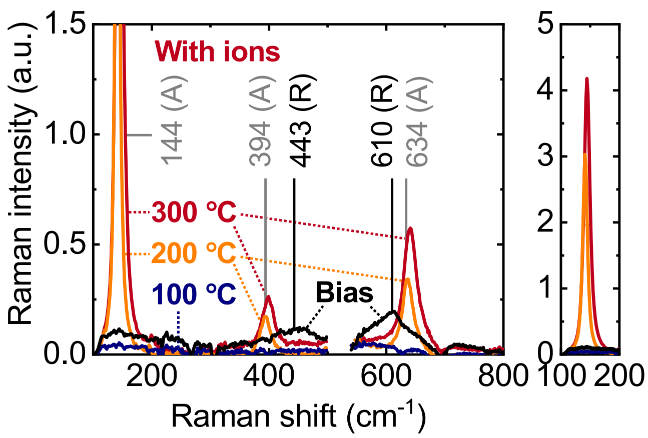

Figure 5. Substrate-corrected Raman spectra of TiO_2 films grown with exposure to ions, at table temperatures of 100, 200, and 300 °C, using a grounded substrate (mean ion energy of 9 ± 1 eV) and plasma steps of 38 s. Additionally, one film is grown at 200 °C using 60 W substrate biasing (mean ion energy of ~120 eV) and plasma steps of 12 s. All spectra are normalized to the 302 cm^{-1} peak of the silicon substrate (see the Supporting Information). Peaks corresponding to the anatase (A) and rutile (R) phase of TiO_2 are indicated.[30,40]

ion-exposed regions of the LHAR structures and serve as a benchmark for the TiO_2 grown without exposure to ions (discussed in Figure 6). For the purpose of comparing different measurements, all Raman spectra are normalized to the 302 cm^{-1} peak of the silicon substrate, of which the signal is subtracted from the data (see the Supporting Information). Peaks corresponding to the anatase phase of TiO_2 are obtained for depositions at a table temperature of 200 and 300 °C, while peaks corresponding to rutile TiO_2 are measured for the film grown with substrate biasing using a table temperature of 200 °C. An almost negligible Raman signal is obtained when using a table temperature of 100 °C, indicating a predominantly amorphous film. These observations are in good agreement with results reported in the literature.[5,17,19,30,38,39]

To probe the crystallinity of the TiO_2 grown with and without exposure to ions, the Raman measurements presented

https://doi.org/10.1021/acs.chemmater.1c00781
Chem. Mater. 2021, 33, 5002−5009

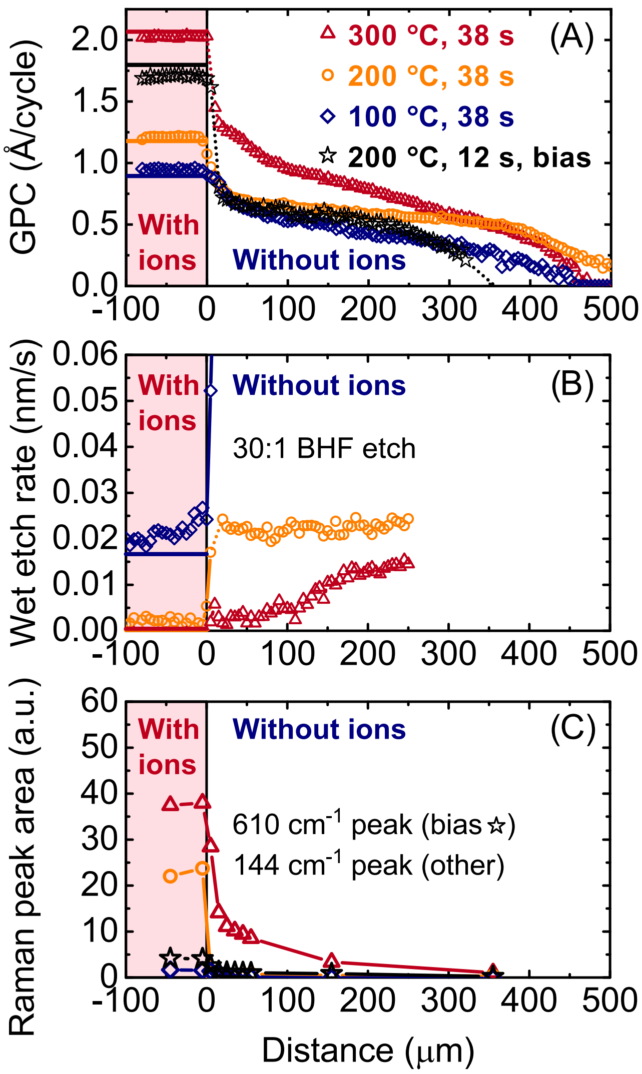

Figure 6. Local GPC, wet etch rate, and Raman peak area (at 144 or 610 cm^{-1}) of TiO_2 films grown using 400 cycles on LHAR cavity structures, indicating a significantly higher GPC, wet etch resistance, and crystallinity in the region where the TiO_2 is grown with exposure to ions (left). The GPC and wet etch rate values obtained with exposure to ions are confirmed by spectroscopic ellipsometry (horizontal bars). The wet etch rate data obtained at 200 °C with substrate biasing (not shown here) are similar to those obtained with a grounded substrate (see the Supporting Information). At 100 °C, the film grown without exposure to ions was fully etched, corresponding to a wet etch rate of ≥0.05 nm s^{-1}.

in Figure 5 have been performed in the ion-exposed and ion-shielded regions of the LHAR structures. The results are summarized in panel C of Figure 6, where the area of the normalized 144 cm^{-1} peak for anatase TiO_2 or 610 cm^{-1} peak for rutile TiO_2 is plotted as a function of distance into the cavity. This peak area gives a measure for the level of crystallinity, which can, for instance, be amorphous (negligible signal), mixed-phase (low signal), or fully crystalline (high signal), although other aspects such as crystal size could also play a role. Furthermore, the Raman signals are compared with the local GPC in terms of thickness (panel A) and the local wet etch rate in 30:1 buffered HF (panel B).

The Raman data given in Figure 6 indicate that predominantly crystalline TiO_2 is grown at 200 and 300 °C with exposure to ions, while the Raman signal strongly decreases in the region where the TiO_2 is grown without any contribution of ions. Correspondingly, at 200 and 300 °C, the wet etch rate is negligible in the ion-exposed region (as confirmed by spectroscopic ellipsometry) but is considerably higher (~0.02 nm s^{-1}) in the ion-shielded region. A somewhat similar but less pronounced effect is observed for plasma ALD of SiO_2, where the wet etch rate reduces up to a factor of ~10 upon exposure to ions.[16] At 300 °C, the Raman signal is also significant in the ion-shielded region, indicating that the thermal energy alone was sufficient for crystallization. The gradual decrease in the Raman signal with distance into the cavity (and corresponding increase in the wet etch rate) could be a thickness effect since complete film crystallization typically only happens after reaching a certain film thickness (here, all films were grown using 400 cycles).[23,30,31,41−43] Moreover, since a higher GPC is obtained for crystalline TiO_2 (as further discussed below),[19,31] this gradual decrease in crystallinity could have enhanced the decrease in GPC with distance into the cavity acquired at 300 °C. Finally, at 100 °C, an almost negligible Raman signal and a significant wet etch rate of ~0.02 nm s^{-1} is obtained in the ion-exposed region, while the Raman signal goes to zero and the wet etch rate strongly increases to ≥0.05 nm s^{-1} in the ion-shielded region (where the film was completely etched).

In addition to the wet etch rate, the Raman signal is also correlated with the GPC. A considerably higher average GPC is obtained for the crystalline (anatase or rutile) films compared to the amorphous films. This impact of crystallinity on the GPC during plasma ALD of TiO_2 has also been reported in the literature[19,31] and may be related to the difference in the surface morphology[19,30,31,38] and microstructure between amorphous, anatase, and rutile TiO_2 (see the Supporting Information for scanning electron microscopy (SEM) images of the TiO_2 surface). The increase in GPC in the ion-exposed region is even larger for the deposition carried out using substrate biasing. Since substrate biasing primarily influences the ion energy,[20] this result supports that the observed effects are indeed caused by ions. Other effects are expected to be of less influence, such as the potential influence of photons (e.g., UV-induced surface hydroxylation[44]), a thermal growth component during the plasma half-cycle,[28] and soft-saturation during the precursor step, where decomposition of $Ti(NMe_2)_4$ may be significant at high temperatures (e.g., at 300 °C).[45]

By the aforementioned results it is concluded that, also under mild plasma conditions, ions have a strong impact on the film crystallinity and GPC during plasma ALD of TiO_2. Since the flux and energy of ions is dependent on the plasma source design and plasma conditions employed, this strong impact of ions could (partly) explain the limited process reproducibility and large spread in GPC values reported for TiO_2 in the literature,[19,21−29] which appears to be a long-standing issue. To better control the growth of TiO_2 thin films by plasma ALD, it is therefore important to gain detailed information on the influence of ions under various conditions. This is further explored in Figure 7, which summarizes data of TiO_2 films grown on LHAR structures with and without exposure to ions, using different plasma exposure times and temperature setpoints of 100, 200, and 300 °C (see the Supporting Information for the measured thickness profiles).

Figure 7 shows that the plasma exposure time, which sets the dose of ions, has a different influence depending on the deposition temperature. For example, at 100 °C, the refractive

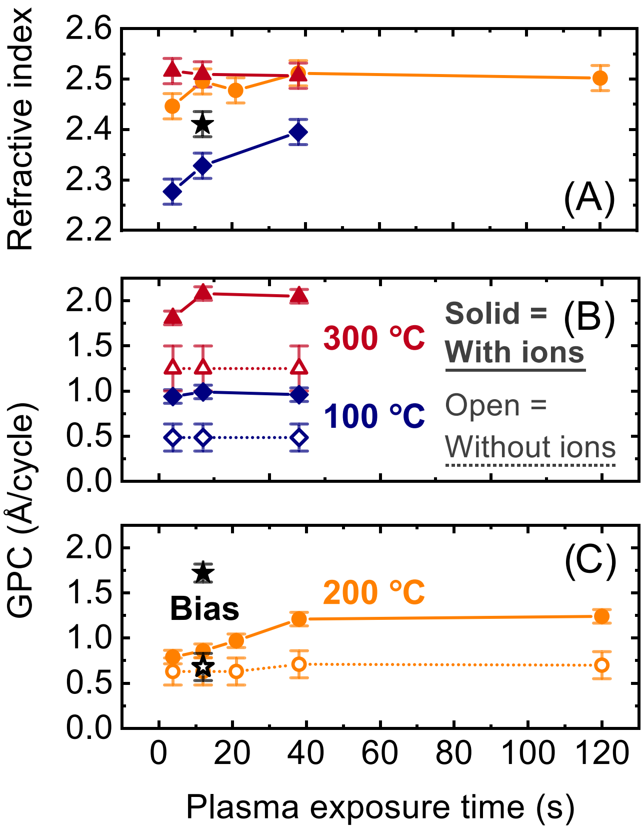

Figure 7. Refractive index at 633 nm (panel A) and GPC values (panels B and C) of TiO_2 films grown with exposure to ions (solid symbols) and without ions (open symbols), at temperature setpoints of 100 and 300 °C (grounded substrate) and at 200 °C (grounded and biased substrates). The refractive indices are measured by spectroscopic ellipsometry on Si reference samples. The GPCs are determined using reflectometry on LHAR structures, as shown in Figures 3 and 4, where the values obtained with ions are confirmed by spectroscopic ellipsometry (see the Supporting Information).

index (at 633 nm) significantly increases when using longer plasma steps (while the band gap remains similar, see the Supporting Information). This suggests densification of the predominantly amorphous TiO_2 grown at 100 °C. In contrast, at 300 °C, the refractive index of the (anatase) TiO_2 is relatively constant and the GPC slightly increases with plasma exposure time. A minor increase in the refractive index is observed at 200 °C, which is correlated with a strong increase in the Raman peak area (see the Supporting Information) and an increase in the difference in GPC with and without ions. Specifically, a difference $GPC_{\text{with ions}} - GPC_{\text{without ions}}$ of approximately 0.15 Å/cycle is obtained when using plasma steps of 3.8 s, which increases to approximately 0.5 Å/cycle when using plasma steps of 38 s or 120 s.

The results obtained at 200 °C illustrate that the plasma exposure time is a parameter that can be used to either limit or exploit the influence of ions. As demonstrated by Faraz et al.,[20] also for plasma ALD of TiO_2, the influence of ions can be described and tuned in a more universal way in terms of the ion-energy dose, i.e., the mean ion energy × ion flux × plasma exposure time.[16,20] In Figure 7, the different plasma exposure times corresponded to an ion-energy dose of ~3 eV nm^{-2} $cycle^{-1}$ (3.8 s plasma) up to ~110 eV nm^{-2} $cycle^{-1}$ (120 s plasma), as calculated using the RFEA measurement given in Figure 2. At 200 °C, the influence of ions was therefore still moderate at ~3 eV nm^{-2} $cycle^{-1}$ and appeared to have reached a maximum at ~110 eV nm^{-2} $cycle^{-1}$. On the basis of these results, it is expected that an ion-energy dose of ~1 eV nm^{-2} $cycle^{-1}$ or lower should be used to limit the influence of ions during plasma ALD of TiO_2. A high plasma pressure, giving a more collisional plasma sheath and a wider ion angle distribution,[46] could also help in obtaining uniform growth on a 3D surface topography. On the other hand, a high ion-energy dose of ~100 eV nm^{-2} $cycle^{-1}$ can be used to exploit the influence of ions, for instance, for tailoring material properties and for emerging methods such as topographically selective processing.[19,47]

CONCLUSIONS

In conclusion, we have demonstrated that ions, including ions with a low energy of <20 eV, have a strong impact on the growth of TiO_2 thin films by plasma ALD. Notably, it was observed that the GPC can increase by ~20 to >200% under the influence of ions, even under common conditions such as a mild plasma and when using a grounded substrate. Because the flux of ions is directional, this influence has a strong impact on the film conformality obtained on 3D nanostructures. Moreover, since conformal growth up to extremely high AR values of ~500 was achieved by a flux of reactive neutrals only, the influence of ions on film conformality is dominant in the case of plasma ALD of TiO_2 under the conditions employed. The impact of ions on the GPC was observed to be related to ion-induced crystallization, which led to a strong reduction in the wet etch rate. Moreover, the magnitude of this impact was found to be dependent on multiple parameters such as temperature, plasma exposure time, and ion energy. These results can serve as guidelines for limiting or exploiting the influence of ions. For example, in this work, relatively little influence of ions was observed at 200 °C when using short plasma steps and a grounded substrate (giving a low ion-energy dose of ~1 eV nm^{-2} $cycle^{-1}$), while the largest effect was obtained when using extended plasma exposures or substrate biasing (~100 eV nm^{-2} $cycle^{-1}$). These are important insights for advancing the level of control over plasma ALD of TiO_2, in terms of film conformality, material properties, and process reproducibility.

ASSOCIATED CONTENT

Supporting Information

The Supporting Information is available free of charge at https://pubs.acs.org/doi/10.1021/acs.chemmater.1c00781.

GPC values reported in the literature for plasma ALD of TiO_2 using $Ti(NMe_2)_4$; further details on the reflectometry, spectroscopic ellipsometry, and Raman spectroscopy measurements; and additional supporting data (overview of measured thickness profiles and dielectric functions, wet etch rate data for TiO_2 grown with substrate biasing, Raman spectroscopy data for TiO_2 grown at 200 °C using different plasma exposure times, and SEM images of TiO_2 films grown at 100, 200, and 300 °C) (PDF)

AUTHOR INFORMATION

Corresponding Authors

Wilhelmus M. M. Kessels − *Eindhoven University of Technology, 5600 MB Eindhoven, The Netherlands;*

orcid.org/0000-0002-7630-8226;
Email: w.m.m.kessels@tue.nl

Harm C. M. Knoops – *Eindhoven University of Technology, 5600 MB Eindhoven, The Netherlands; Oxford Instruments Plasma Technology, Bristol BS49 4AP, United Kingdom;* orcid.org/0000-0003-2284-4477;
Email: h.c.m.knoops@tue.nl

Authors

Karsten Arts – *Eindhoven University of Technology, 5600 MB Eindhoven, The Netherlands;* orcid.org/0000-0003-4266-6559

Harvey Thepass – *Eindhoven University of Technology, 5600 MB Eindhoven, The Netherlands*

Marcel A. Verheijen – *Eindhoven University of Technology, 5600 MB Eindhoven, The Netherlands; Eurofins Material Science, 5656 AE Eindhoven, The Netherlands*

Riikka L. Puurunen – *Aalto University School of Chemical Engineering, FI-00076 Aalto, Finland;* orcid.org/0000-0001-8722-4864

Complete contact information is available at:
https://pubs.acs.org/10.1021/acs.chemmater.1c00781

Notes

The authors declare no competing financial interest.

■ ACKNOWLEDGMENTS

This work was part of the research program HTSM with Project No. 15352, which is (partly) financed by the Netherlands Organization for Scientific Research (NWO). R.L.P acknowledges funding from Academy of Finland, ALDI project, decision no. 331082. VTT Technical Research Centre of Finland Ltd. and Dr. M. Utriainen are acknowledged for supplying the PillarHall LHAR4 conformality test structures. Lam Research Corp. is acknowledged for providing the vertical trench nanostructures. Solliance and the Dutch province of Noord Brabant are acknowledged for funding the TEM facility. The authors thank Dr. B. Barcones Campo for the FIB preparation of the TEM sample. Finally, C. van Helvoirt, P. Bax, and W. J. H.Berghuis are thanked for their technical support.

■ REFERENCES

(1) Chen, X.; Mao, S. S. Titanium Dioxide Nanomaterials: Synthesis, Properties, Modifications and Applications. *Chem. Rev.* **2007**, *107*, 2891–2959.

(2) Fujishima, A.; Zhang, X.; Tryk, D. A. TiO2 Photocatalysis and Related Surface Phenomena. *Surf. Sci. Rep.* **2008**, *63*, 515–582.

(3) Yu, J.; Lei, J.; Wang, L.; Zhang, J.; Liu, Y. TiO2 Inverse Opal Photonic Crystals: Synthesis, Modification, and Applications - A Review. *J. Alloys Compd.* **2018**, *769*, 740–757.

(4) Szeghalmi, A.; Helgert, M.; Brunner, R.; Heyroth, F.; Gösele, U.; Knez, M. Atomic Layer Deposition of Al2O3 and Ti02 Multilayers for Applications as Bandpass Filters and Antireflection Coatings. *Appl. Opt.* **2009**, *48*, 1727–1732.

(5) Ghazaryan, L.; Handa, S.; Schmitt, P.; Beladiya, V.; Roddatis, V.; Tünnermann, A.; Szeghalmi, A. Structural, Optical, and Mechanical Properties of TiO2 Nanolaminates. *Nanotechnology* **2021**, *32*, No. 095709.

(6) O'Regan, B.; Grätzel, M. A Low-Cost, High-Efficiency Solar Cell Based on Dye-Sensitized Colloidal Ti02 Films. *Nature* **1991**, *353*, 737–740.

(7) Kim, S. K.; Choi, G. J.; Lee, S. Y.; Seo, M.; Lee, S. W.; Han, J. H.; Ahn, H. S.; Han, S.; Hwang, C. S. Al-Doped TiO2 Films with Ultralow Leakage Currents for next Generation DRAM Capacitors. *Adv. Mater.* **2008**, *20*, 1429–1435.

(8) George, S. M. Atomic Layer Deposition: An Overview. *Chem. Rev.* **2010**, *110*, 111–131.

(9) Profijt, H. B.; Potts, S. E.; van de Sanden, M. C. M.; Kessels, W. M. M. Plasma-Assisted Atomic Layer Deposition: Basics, Opportunities, and Challenges. *J. Vac. Sci. Technol., A* **2011**, *29*, No. 050801.

(10) Knoops, H. C. M.; Faraz, T.; Arts, K.; Kessels, W. M. M. Status and Prospects of Plasma-Assisted Atomic Layer Deposition. *J. Vac. Sci. Technol., A* **2019**, *37*, No. 030902.

(11) Raley, A.; Thibaut, S.; Mohanty, N.; Subhadeep, K.; Nakamura, S.; Ko, A.; O'Meara, D.; Tapily, K.; Consiglio, S.; Biolsi, P. In *Self-Aligned Quadruple Patterning Integration Using Spacer on Spacer Sub-32nm Pitch ApplicationsNanopatterning V*, Advanced Etch Technology for Nanopatterning V, 2016; Vol. 9782.

(12) Dallorto, S.; Staaks, D.; Schwartzberg, A.; Yang, X.; Lee, K. Y.; Rangelow, I. W.; Cabrini, S.; Olynick, D. L. Atomic Layer Deposition for Spacer Defined Double Patterning of Sub-10 Nm Titanium Dioxide Features. *Nanotechnology* **2018**, *29*, No. 405302.

(13) Swaminathan, S.; Pasquale, F. L.; LaVoie, A. Plasma Assisted Atomic Layer Deposition Titanium Oxide for Conformal Encapsulation and Gapfill Applications. U.S. Patent US9,373,500 B22016.

(14) Arts, K.; Utriainen, M.; Puurunen, R. L.; Kessels, W. M. M.; Knoops, H. C. M. Film Conformality and Extracted Recombination Probabilities of O Atoms during Plasma-Assisted Atomic Layer Deposition of SiO2, TiO2, Al2O3, and HfO2. *J. Phys. Chem. C* **2019**, *123*, 27030–27035.

(15) Arts, K.; Deijkers, J. H.; Puurunen, R. L.; Kessels, W. M. M.; Knoops, H. C. M. Oxygen Recombination Probability Data for Plasma-Assisted Atomic Layer Deposition of SiO2 and TiO2. *J. Phys. Chem. C* **2021**, *125*, 8244–8252.

(16) Arts, K.; Deijkers, J. H.; Faraz, T.; Puurunen, R. L.; Kessels, W. M. M.; Knoops, H. C. M. Evidence for Low-Energy Ions Influencing Plasma-Assisted Atomic Layer Deposition of SiO2: Impact on the Growth per Cycle and Wet Etch Rate. *Appl. Phys. Lett.* **2020**, *117*, No. 031602.

(17) Profijt, H. B.; van de Sanden, M. C. M.; Kessels, W. M. M. Substrate Biasing during Plasma-Assisted ALD for Crystalline Phase-Control of TiO2 Thin Films. *Electrochem. Solid-State Lett.* **2011**, *15*, No. G1.

(18) Profijt, H. B.; van de Sanden, M. C. M.; Kessels, W. M. M. Substrate-Biasing during Plasma-Assisted Atomic Layer Deposition to Tailor Metal-Oxide Thin Film Growth. *J. Vac. Sci. Technol., A* **2013**, *31*, No. 01A106.

(19) Faraz, T.; Knoops, H. C. M.; Verheijen, M. A.; van Helvoirt, C. A. A.; Karwal, S.; Sharma, A.; Beladiya, V.; Szeghalmi, A.; Hausmann, D. M.; Henri, J.; et al. Tuning Material Properties of Oxides and Nitrides by Substrate Biasing during Plasma-Enhanced Atomic Layer Deposition on Planar and 3D Substrate Topographies. *ACS Appl. Mater. Interfaces* **2018**, *10*, 13158–13180.

(20) Faraz, T.; Arts, K.; Karwal, S.; Knoops, H. C. M.; Kessels, W. M. M. Energetic Ions during Plasma-Enhanced Atomic Layer Deposition and Their Role in Tailoring Material Properties. *Plasma Sources Sci. Technol.* **2019**, *28*, No. 024002.

(21) Park, J.-J.; Lee, W.-J.; Lee, G.-H.; Kim, I.-S.; Shin, B.-C.; Yoon, S.-G. Very Thin TiO_2 Films Prepared by Plasma Enhanced Atomic Layer Deposition (PEALD). *Integr. Ferroelectr.* **2004**, *68*, 129–137.

(22) Kim, W.-S.; Ko, M.-G.; Kim, T.-S.; Park, S.-K.; Moon, Y.-K.; Lee, S.-H.; Park, J.-G.; Park, J.-W. Titanium Dioxide Thin Films Deposited by Plasma Enhanced Atomic Layer Deposition for OLED Passivation. *J. Nanosci. Nanotechnol.* **2008**, *8*, 4726–4729.

(23) Xie, Q.; Musschoot, J.; Deduytsche, D.; Van Meirhaeghe, R. L.; Detavernier, C.; Van den Berghe, S.; Jiang, Y.-L.; Ru, G.-P.; Li, B.-Z.; Qu, X.-P. Growth Kinetics and Crystallization Behavior of TiO2 Films Prepared by Plasma Enhanced Atomic Layer Deposition. *J. Electrochem. Soc.* **2008**, *155*, No. H688.

(24) Lee, C.-S.; Kim, J.; Gu, G. H.; Jo, D.-H.; Park, C. G.; Choi, W.; Kim, H. Photocatalytic Activities of TiO2 Thin Films Prepared on

Galvanized Iron Substrate by Plasma-Enhanced Atomic Layer Deposition. *Thin Solid Films* **2010**, *518*, 4757−4761.
(25) Kang, B.-W.; Kim, W.-S.; Hwang, C.-M.; Moon, D.-Y.; Kim, J.-J.; Park, J.-G.; Park, J.-W. Titanium Oxide Thin Films Prepared by Plasma Enhanced Atomic Layer Deposition Using Remote Electron Cyclotron Resonance Plasma for Organic Devices Passivation. *Jpn. J. Appl. Phys.* **2010**, *49*, No. 08JG05.
(26) Jin, M.-J.; Jo, J.; Kim, J.-H.; An, K.-S.; Jeong, M. S.; Kim, J.; Yoo, J.-W. Effects of TiO2 Interfacial Atomic Layers on Device Performances and Exciton Dynamics in ZnO Nanorod Polymer Solar Cells. *ACS Appl. Mater. Interfaces* **2014**, *6*, 11649−11656.
(27) Schindler, P.; Logar, M.; Provine, J.; Prinz, F. B. Enhanced Step Coverage of TiO2 Deposited on High Aspect Ratio Surfaces by Plasma-Enhanced Atomic Layer Deposition. *Langmuir* **2015**, *31*, 5057−5062.
(28) Provine, J.; Schindler, P.; Torgersen, J.; Kim, H. J.; Karnthaler, H.-P.; Prinz, F. B. Atomic Layer Deposition by Reaction of Molecular Oxygen with Tetrakisdimethylamido-Metal Precursors. *J. Vac. Sci. Technol., A* **2016**, *34*, No. 01A138.
(29) Vandenbroucke, S. S. T.; Levrau, E.; Minjauw, M. M.; Van Daele, M.; Solano, E.; Vos, R.; Dendooven, J.; Detavernier, C. Study of the Surface Species during Thermal and Plasma-Enhanced Atomic Layer Deposition of Titanium Oxide Films Using in Situ IR-Spectroscopy and in Vacuo X-Ray Photoelectron Spectroscopy. *Phys. Chem. Chem. Phys.* **2020**, *22*, 9262−9271.
(30) Ratzsch, S.; Kley, E. B.; Tünnermann, A.; Szeghalmi, A. Influence of the Oxygen Plasma Parameters on the Atomic Layer Deposition of Titanium Dioxide. *Nanotechnology* **2015**, *26*, No. 024003.
(31) Langereis, E.; Heil, S. B. S.; Knoops, H. C. M.; Keuning, W.; Van De Sanden, M. C. M.; Kessels, W. M. M. In Situ Spectroscopic Ellipsometry as a Versatile Tool for Studying Atomic Layer Deposition. *J. Phys. D: Appl. Phys.* **2009**, *42*, No. 073001.
(32) Gao, F.; Arpiainen, S.; Puurunen, R. L. Microscopic Silicon-Based Lateral High-Aspect-Ratio Structures for Thin Film Conformality Analysis. *J. Vac. Sci. Technol., A* **2015**, *33*, No. 010601.
(33) Yim, J.; Ylivaara, O. M. E.; Ylilammi, M.; Korpelainen, V.; Haimi, E.; Verkama, E.; Utriainen, M.; Puurunen, R. L. Saturation Profile Based Conformality Analysis for Atomic Layer Deposition: Aluminum Oxide in Lateral High-Aspect-Ratio Channels. *Phys. Chem. Chem. Phys.* **2020**, *22*, 23107−23120.
(34) Puurunen, R. L.; Gao, F. In *Influence of ALD Temperature on Thin Film Conformality: Investigation with Microscopic Lateral High-Aspect-Ratio Structures*, 14th International Baltic Conference on Atomic Layer Deposition, 2016; pp 20−24.
(35) Sharma, A.; Longo, V.; Verheijen, M. A.; Bol, A. A.; Kessels, W. M. M. Erwin. Atomic Layer Deposition of HfO2 Using HfCp-(NMe2)3 and O2 Plasma. *J. Vac. Sci. Technol., A* **2017**, *35*, No. 01B130.
(36) Heil, S. B. S.; van Hemmen, J. L.; Hodson, C. J.; Singh, N.; Klootwijk, J. H.; Roozeboom, F.; van de Sanden, M. C. M.; Kessels, W. M. M. Deposition of TiN and HfO2 in a Commercial 200 Mm Remote Plasma Atomic Layer Deposition Reactor. *J. Vac. Sci. Technol., A* **2007**, *25*, 1357−1366.
(37) Knoops, H. C. M.; Langereis, E.; van de Sanden, M. C. M.; Kessels, W. M. M. Conformality of Plasma-Assisted ALD: Physical Processes and Modeling. *J. Electrochem. Soc.* **2010**, *157*, No. G241.
(38) Chiappim, W.; Testoni, G. E.; Doria, A. C. O. C.; Pessoa, R. S.; Fraga, M. A.; Galvão, N. K. A. M.; Grigorov, K. G.; Vieira, L.; Maciel, H. S. Relationships among Growth Mechanism, Structure and Morphology of PEALD TiO2 Films: The Influence of O2 Plasma Power, Precursor Chemistry and Plasma Exposure Mode. *Nanotechnology* **2016**, *27*, No. 305701.
(39) Avila, J. R.; Qadri, S. B.; Freitas, J. A.; Nepal, N.; Boris, D. R.; Walton, S. G.; Eddy, C. R.; Wheeler, V. D. Impact of Growth Conditions on the Phase Selectivity and Epitaxial Quality of TiO2 Films Grown by the Plasma-Assisted Atomic Layer Deposition. *Chem. Mater.* **2019**, *31*, 3900−3908.
(40) Hardcastle, F. Raman Spectroscopy of Titania (TiO2) Nanotubular Water-Splitting Catalysts. *J. Arkansas Acad. Sci.* **2011**, *65*, No. 1.
(41) Lee, S.; Noh, W.; Kim, H. In *Effect of Ligand Structure on Crystallinity of Atomic Layer Deposited TiO2*, The AVS 20th International Conference on Atomic Layer Deposition, 2020.
(42) Oh, I.-K.; Zeng, L.; Kim, J. E.; Park, J. S.; Kim, K.; Lee, H.; Seo, S.; Khan, M. R.; Kim, S.; Park, C. W.; et al. Surface Energy Change of Atomic-Scale Metal Oxide Thin Films by Phase Transformation. *ACS Nano* **2020**, *14*, 676−687.
(43) Puurunen, R. L.; Sajavaara, T.; Santala, E.; Miikkulainen, V.; Saukkonen, T.; Laitinen, M.; Leskelä, M. Controlling the Crystallinity and Roughness of Atomic Layer Deposited Titanium Dioxide Films. *J. Nanosci. Nanotechnol.* **2011**, *11*, 8101−8107.
(44) Sun, J.; Guo, L. H.; Zhang, H.; Zhao, L. UV Irradiation Induced Transformation of TiO2 Nanoparticles in Water: Aggregation and Photoreactivity. *Environ. Sci. Technol.* **2014**, *48*, 11962−11968.
(45) Yun, J. Y.; Park, M. Y.; Rhee, S. W. Comparison of Tetrakis(Dimethylamido)Titanium and Tetrakis(Diethylamido)Titanium as Precursors for Metallorganic Chemical Vapor Deposition of Titanium Nitride. *J. Electrochem. Soc.* **1999**, *146*, 1804−1808.
(46) Mizutani, N.; Hayashi, T. Ion Energy and Angular Distribution at the Radio Frequency Biased Electrode in an Inductively Coupled Plasma Apparatus. *J. Vac. Sci. Technol., A* **2001**, *19*, 1298−1303.
(47) Vallée, C.; Bonvalot, M.; Belahcen, S.; Yeghoyan, T.; Jaffal, M.; Vallat, R.; Chaker, A.; Lefèvre, G.; David, S.; Bsiesy, A.; et al. Plasma Deposition—Impact of Ions in Plasma Enhanced Chemical Vapor Deposition, Plasma Enhanced Atomic Layer Deposition, and Applications to Area Selective Deposition. *J. Vac. Sci. Technol., A* **2020**, *38*, No. 033007.